Proceedings of the ASME 2009 International Mechanical Engineering Congress & Exposition
IMECE2009
November 13-19, Lake Buena Vista, Florida, USA

IMECE2009-12318

NANO-ENGINEERING SILICA AEROGEL STRUCTURE TO DETERMINE THE PROPERTY-STRUCTURE RELATIONSHIP

Gitogo Churu
School of Mechanical and Energy Engineering
University of North Texas
Denton, Texas, USA

Hongbing Lu
School of Mechanical and Energy Engineering
University of North Texas
Denton, Texas, USA

Nicholas Leventis
Missouri University of Science
and Technology
Rolla, Missouri, USA

ABSTRACT

We characterize mechanically strong nano/meso-porous cross-linked templated silica aerogels that were synthesized through the sol gel process and reinforced by nano casting a 4-10nm thick conformal layer of isocynate derived polymer. Tri-block co-polymer (pluronic P123) was used as a structure directing agent to produce ordered mesoporous walls while 1, 3, 5 trimethylbenzene (TMB) was added as micelle-swelling reagent to regulate the size of the pores. The shape and size of the micro and meso pores were nano engineered by varying the amount of chemical surfactant as well as the concentration of the cross-linking solution used to form the polymer nano layer. In so doing we manipulated the structure at the molecular level to develop an optimized structure that closely resembles the honeycomb structure found in nature. Dynamic mechanical analysis (DMA) test results established that the material had an α-grass transition temperature of about 130°C while quasi-static compression tests showed that the optimized nano-structured silica aerogel had a Young's modulus of about 800MPa. We present the synthesis protocol as well as chemical, physical and mechanical characterization of cross-linked templated silica aerogel (CTSA).). In addition, material point method (MPM) simulation results are highlighted.

NOMENCLATURE

Cross-linked template silica aerogel, MPM, DMA test

INTRODUCTION

Aerogels are low density porous nano-structured materials with low thermal conductivity as well as high acoustic impedance. So far, however, their inherent fragility limits their application to only specialized environments such as collectors of hypervelocity particles in space and as thermal insulator on planetary vehicles in mars and as Cherenkov radiation detectors in certain types of nuclear reactors. Mass production of aerogels is further complicated by the need to use supercritical drying, a process that is both expensive and size limiting.

We present here the results of one class of aerogel, the cross-linked templated silica aerogels (CTSA) that were prepared through the sol gel process and dried in ambient condition using pentane as the solvent exchange fluid. CTSA are similar to materials first developed by Mobil Corporation in 1992, and classified as M41S [1] which ware characterized as a series of ordered mesoporous silica with uniform pore size and large surface area. Their pore sizes were 20-30Å and were synthesized using micelles of cationic

surfactant as templates in a base-catalyzed protocol. Consecutive developments by Stucky [2] introduced large copolymers (Pluronic 123) as templating agent to produce SBA class of materials with pore sizes up to 300Å. Addition of TMB as swelling surfactant increased the pores further [3].

Earlier we published results of polymer nano-encapsulated templated mesoporous silica aerogels that had improved mechanical properties than earlier reported [4]. The samples used in that work had been dried using supercritical drying, a process that limited the size of the samples that could be made because of the small size of the high pressure autocrave used in supercritical drying. Instead of the CO_2 used in supercritical drying, a solvent with low surface tension (pentane) was used as an exchange fluid and then samples were dried in the ambient conditions to produce samples identical to those dried supercritically.

1. EXPERIMENTAL: MATERIALS AND SAMPLE PREPARATION

CTSA wet gels were made using well established procedure [3, 4]. All chemicals and materials used were commercially obtained and use without any further purification. Pluronic P123, TMOS and TMB were purchased from Sigma Aldridge (St. Louis MO, 63103), Nitric acid was purchased from Fisher chemicals/Fisher scientific, (Pittsburgh, PA 15275), while acetone, dry alcohol and acetonitrile were purchased from Pharmco—AAPER chemicals and commercial alcohols, (Shelbyville KY, 40065). Research samples of Hexamethylene-1, 6 diisocyanate (Desmodur N3200) used for cross-linking were donated by Bayer material science, (Pittsburgh, PA 15205), while 10 ml Syringes used as molds for the compression samples were purchased from BD syringes, (Franklin Lakes NJ 07417)

4gm of pluronic P123 was dissolved in 12gm of 1.0M HNO3 to make a chemical template. An amount of TMB was added as a structure directing surfactant and was varied to create different structures. After cooling the mixture to 0°C, 5.15gm of tetraorthosilacate (TMOS) was added and the mixture was allowed to gel and age at 60°C for about 10 hours. There after the samples were washed in dry alcohol to remove water followed by acetone wash. Cross-linking was then done by placing the samples in a solution of 11gm of N3200 dissolved in 94ml of acetone and then curing at 55°C for 36 hours. Upon washing with acetone to remove excess N3200, the samples were washed with pentane and dried in ambient condition. For comparison, some samples were dried in a supercritical dryer.

2. RESULTS AND DISCUSSION

Scanning electron microscopy (SEM) imaging was done to map the resulting micro structure. It was established that as TMB was varied from 0gm to 3.1gm, the shape of the pores changed from random disorganized mass [fig.1] to well defined honeycomb like structure when 0.45gm of TMB was used[fig.2]. Any addition of the structure directing TMB resulted in more disorder [fig. 3 E, F, G) and finally mesoporous foam resulted at very high concentration of TMB [fig.3 H]. Brunauer-Emmett-Teller (BET) analysis [table1] showed that the material retained porosity above 47%, while confirming the similarity between pentane dried samples with those dried using the traditional supercritical drying process.

Quasi-static compression test were conducted in accordance to ASTM standard D695-2a to establish the basic mechanical properties such as Young's modulus as well as yield strength of the material. Figure 4 shows compression results of native (uncross-linked) samples. They were brittle and fragmented at low strain (below 5%) upon compression. Once they were cross-linked with 11gm of N3200 dissolved in 94ml of acetone, they became more ductile [fig.5]. At low strain (below 5%), the stress – strain curve was linear, followed by

compaction to about 60% strain where there was very small lateral increase in diameter as the material was simply occupying the voids in the meso porosity. Above 60% there was densification before final failure at about 80%. The specific energy absorption of the material was also computed and tabulated in table 2 together with a summary of the other mechanical properties such as yield strength and Young's modulus. Figure 6 shows that there was significant change in Young's modulus with TMB concentration even as the density of the samples remained fairly stable. The optimized structure was obtained when 0.45gm of TMB (X-MP4-T45) was used resulting in a material that had a yield strength of 33MPa and Young's modulus of about 800MPA. In addition, the specific energy absorption was found to be about 121 J/cm^3.

Complex modulus was investigated using 65mm long, 13mm wide and 2mm thick specimens machined from 6" X 3" samples that had been prepared as previously described. They were polished using fine grade sand paper to remove any tool mark left by the end mill used to get the final shape. A model RSA II dynamic mechanical analyzer (Rheumatics Scientific Inc. Piscataway, NJ) was used to conduct DMA tests at University of Oklahoma (Norman, Ok). Each sample was loaded on the knife support of the test chamber and the loading was applied at the mid-span of the sample which now behaved as a simply supported beam. A load of 10 grams was introduced at the mid-span to make sure that the specimen was always in contact with the knife-loading fixture when oscillating load was applied. The frequency was set at 1Hz and then liquid nitrogen was introduced into the chamber to cool the sample to the lower limit of -122°C while the upper temperature limit was set at 250°C. Data sampling was then set at every two minutes and the specimens ware soaked for 20 seconds before recording the data. The loss modulus, the storage modulus as well as tan delta were all recorded simultaneously at each temperature set and are as shown in figure 7. Two peaks, the first at -50°C indicating the β-glass transition, while the other one at about 130°C indicate the α-glass transition temperature. At temperatures above 150°C, there was slight shrinkage of about 1% but the sample still remained on the knife-edge support showing that the material had high degree of dimensional stability even at temperature well above 130°C, which was the approximate α-glass transition temperature.

3. SIMULATIONS USING MPM

Concurrently the evolution of a cross-linked templated aerogel mesostructure under compression was simulated using the Material Point Method (MPM) on a model generated from X-Ray nano-computed tomographic image [6]. In MPM each voxel information in an X-ray tomography [fig.8] was converted to a material point obtained from the novel three-dimensional (3D) [fig.9] nano-tomography (nano-CT) of cross-linked aerogels to generate a MPM model. A parallel version of MPM code, developed at Oklahoma State University (OSU), has been used to simulate the response of a cross-linked templated aerogels under compression at high strain rates. A long split Hopkinson pressure bar [7] was used to measure stress-strain relationship at high strain rates. Simulation results are compared with experimental data. The results from the simulations show that the MPM can effectively model cross-linked templated silica-aerogel considering its real microstructure, and capture the elastic, compaction and densification behavior of the material and the simulation results agree reasonably well with the experimental results [fig.10]. Simulations also indicate a nearly uniform deformation in the aerogel. Further simulations were conducted to indentify functions of polymer coating and the effect of microstructure. Models with different porosities indicate that the skeletal wall thickness of both the aerogel and the polymer coating affect the local stress

distribution, which in turn might induce different mechanical response under compression. MPM simulations show that the stress-strain behavior of cross-linked templated aerogels under compression follows a power law relation with density (porosity) under deformation up to certain strain levels. That relationship breaks down when deformation is very high.

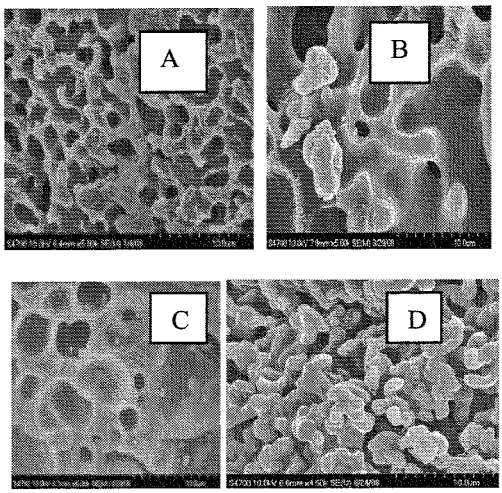

Figure 1: SEM of CTSA with low concentration of TMB at (A) 0gm, 0.1gm(B), 0.2gm (C), and 0.3gm (D)

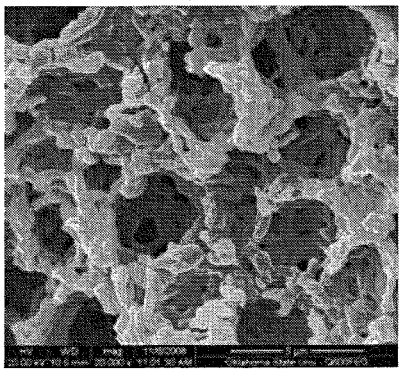

Figure 2: SEM of CTSA when 0.45gm of TMB was used showing a more organized pore structure closely resembling the hone-comb structure.

4. CONCLUSIONS

The close co-relation between nano structure of the material and its mechanical properties was evident. By manipulating the structure of CTSA at the molecular level, we developed structures with varying properties. The porous nature of the resulting material makes them ideal for dual applications where they would be used as load bearing structural applications as well for acoustic and thermal insulation.

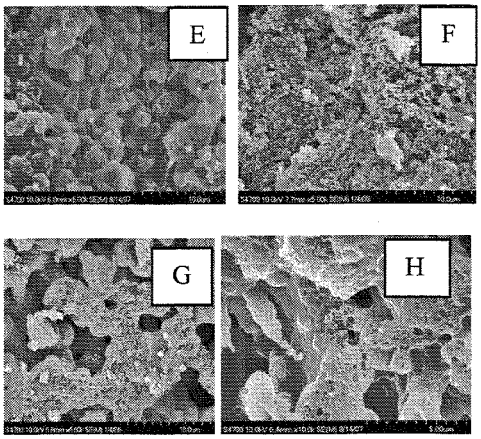

Figure 3: SEM of CTSA with high concentration of TMB with 0.9gm (E), 1.25gm (F), 2.0gm (G), and 3.1gm (H).

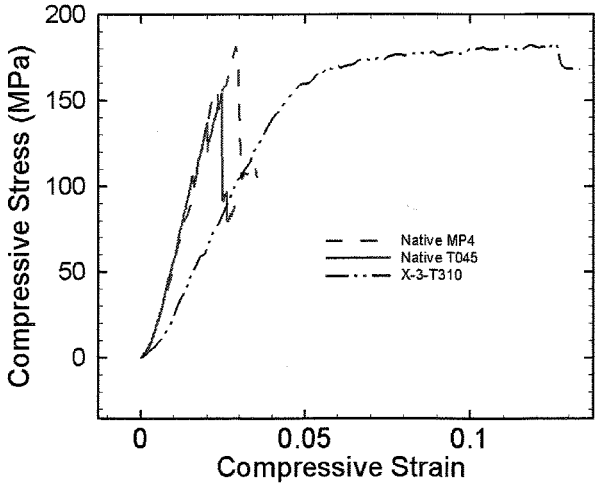

Figure 4: compressive stress strain curves s for samples before cross-linking and one that was lightly cross-linked (X-3-T310).

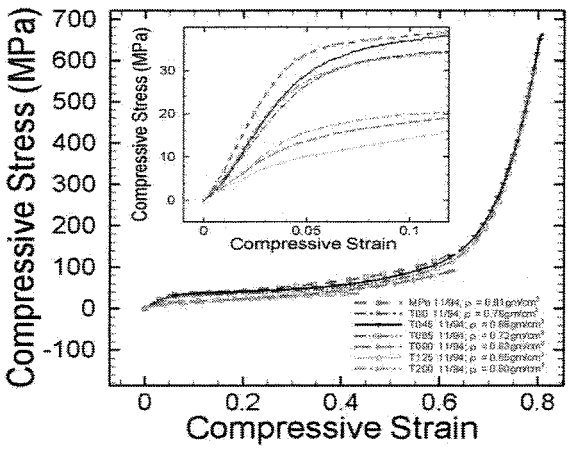

Figure 5: Compressive stress strain curves for cross-linked CTSA with varying amounts of TMB.

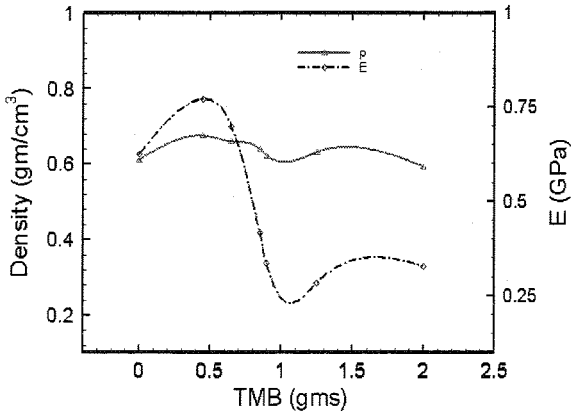

Figure 6: Change in density and Young's Modulus with TMB Concentration

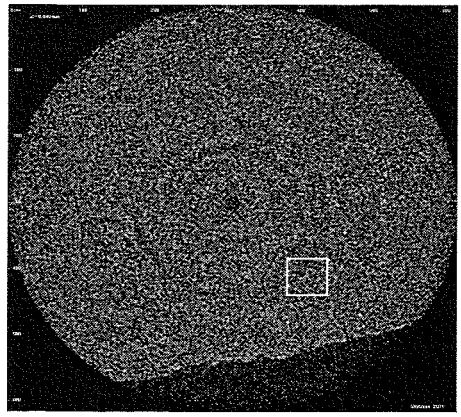

Figure 8: Nano-CT scan for X-MP4-T045 sample used for MPM simulation.

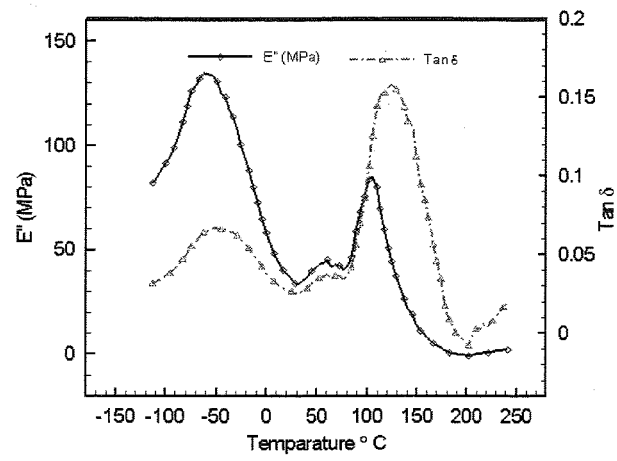

Figure 7: DMA tests showing two distinct picks for α and β grass transition temperatures.

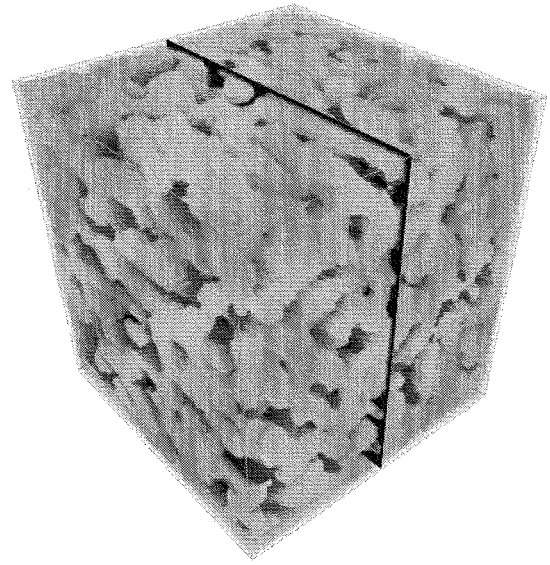

Figure 9: 3D discrete MPM simulation model obtained from nano-CT scan.

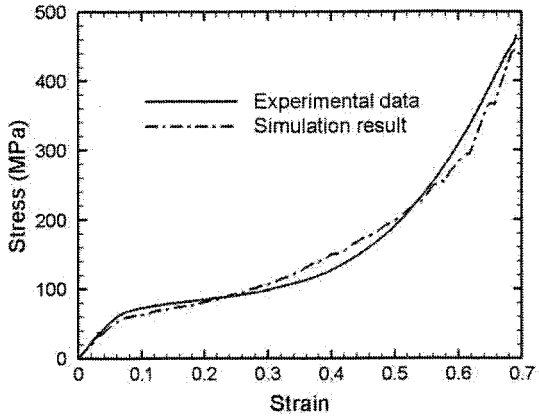

Figure 10: Stress-strain curve at high strain rate ($3070S^{-1}$) comparing experimental data with simulation results.

Table 1: Summary for BET test results

Sample	Bulk density (g/cm^3)	Skeletal Density (g/cm^3)	% Porosity	BET Surface Area [Av. Pore Dia] (m^2g^{-1} [nm])	Pore Dia (nm)
X-MP4-T00 11/94	0.6121	1.335±.0094	54	17.1[11.8]	262.7
X-MP4-T045 11/94(SCF)	0.6752	1.274±0.0016	47	1.61[20.1]	2925.2
X-MP4-T045 11/95(P)	0.6806	1.276±0.0013	47	0.99[300.3]	4751.1
X-MP4-T090 11/94	0.623	1.307±0.001	52	1.43[81.4]	3211..2
X-MP4-T125 11/94	0.6317	1.288±0.0003	66	5.01[44.3]	929.9
X-MP4-T200 11/94	0.5942	1.29±0.0031	54	1.7[50.7]	2735.5

Table 2: Summary of mechanical property data from quasi-static compression tests

Sample	Density (g/cm3)	Young's Modulus (GPa)	Yield Strength (MPa)	Energy density (J/g)	Specific energy density (J/cm3)
X-MP4-T00	0.612±0.019	0 .626±0.004	31.35±0.212	52.14±0.232	85.2
X-MP4-T045	0.69±0.01	0.772±0.0188	33.37±2.189	84.27±0.68	121.74
X-MP4-T065	0.66±0.01	0.700±0.052	22±0	76.5 ±2.5	115.91
X-MP4-T085	0.64±0.01	0.418±0.055	12.5±0.5	70.5±3.5	110.16
X-MP4-T090	0.73±0.01	0.525±0.016	15.6±0.28	84±1 1.2	115.07
X-MP4-T125	0.81±0.02	0.492±0.057	18.5±0.5	100±21.2	123.46
X-MP4-T200	0.67±0.01	0.246±0.032	8.5±0.5	49±1 3.12	71.01

ACKNOWLEDGMENTS
The authors would like to acknowledge support of NSF under CMMI-0653919 and CMMI-0653970.

REFERENCES

[1] Roth, W., Kresge, C., Vartuli, J., Leonowicz, M., Fung, A., McCullen, S., 1995"MCM-36: The First Pillared Molecular Sieve with Zeolite Properties", Studies in Surface Science and Catalysis, Vol. 94.

[2] Kresge, C., Vartuli, J., Roth, W., Leonowicz, M., "The Discovery of ExxonMobil's M41S Family of Mesoporous Molecular Sieves", Studies in Surface Science and catalysis 148.e and Catalysis 148.

[3] Timohiko, A., Kazuki, N., Kazuyuki, H., Tetsuya, K., 2005, "Monolithic Periodic Mesoporous Silica with Well-Defined Macropores," Chem. Mater., 17, pp 2114-2119.

[4] Nicholas, L., Sudhir, M., Xiaojiang, W., Amala, D., Vishal, U. P.,C. Sotiriou-Leventis, Hongbing, L., Gitogo, C., Alex, C., 2008,"Polymer Nano-Encapsulation of Templated Mesoporous Silica Monoliths with Improved Mechanical Properties" Journal of Non-Crystalline Solids Volume 354 (2008) pp 632–644.

[5] Hund, J., Bertino, M., Zhang, G., Sotiriou-Leventis, C., Leventis, N., "Synthesis of homogeneous alloy metal nanoparticles in silica aerogels", 2004, Journal of Non-Crystalline Solids, Volume 350 (2004) pp 9–13.

[6] Daphalapurkar,N., Hanan, J., Phelps, B., Bale, H., Lu, H., 2008, "Tomography and Simulation of Microstructure Evolution of a Closed-Cell Polymer Foam in Compression" Mechanics of Advanced Materials and Structures, Volume 15: pp 594–611.

[7] Luo, H., Churu, G., Fabrizio, F., Schnobrich, J., Hobbs, A., Dass, A., Mulik, S., Zhang, Y., Grady, Capecelatro, P., Sotiriou-Leventis, C., Lu, H., Leventis, N., 2008, "Synthesis and characterization of the physical, chemical and mechanical properties of isocyanate-crosslinked vanadia aerogels" J Sol-Gel Sci Technol (2008) Volume 48: pp 113–134.